

Simplified Modeling of Deflagration in Vessels

Joon Hyun Kim, Joo-Hyun Kim*

School of Mechanical and Automotive Engineering, Kookmin University,
861-1, Chongnung-dong, Songbuk-gu, Seoul 136-702, Korea

A simplified method that models the deflagration process occurring in closed or vented vessels is described. When combustion occurs within the spherical or cylindrical vessels, the flame moves spherically or segmentally to the vessel periphery. The volume and area of each element along the propagating flame front are calculated by using simple geometrical rules. For instabilities and turbulence resulting in enhanced burning rates, a simple analysis results in reasonable agreement with the experimental pressure transients when two burning rates (a laminar burning rate prior to the onset of instability and an enhanced burning rate) were used. Pressure reduction caused by a vent opening at predetermined pressure was modeled. Parameters examined in the modeling include ignition location, mixture concentration, vented area, and vent opening pressure. It was found that venting was effective in reducing the peak pressure experienced in vessels. The model can be expected to estimate reasonable peak pressures and flame front distances by modeling the enhanced burning rates, that is, turbulent enhancement factor.

Key Words : Deflagration, Explosions, Flame, Gas Dynamics

Nomenclature

A : Surface area
 A_v : Vent area
 C_d : Outflow coefficient
 D : Diameter
 H : Enthalpy
 L : Length
 m : Mass
 p : Pressure
 R : Distance to the flame front, $R^2 = s^2 + r^2$
 r : Distance to the flame front touched at the wall
 St : Turbulent burning velocity
 Su : Laminar burning velocity
 s : Radius of cylinder or sphere
 T : Temperature
 t : Time

V : Volume

Greek Symbols

α, β : Empirical parameters
 λ : Specific heat ratio
 ρ : Gas density
 ϕ : Turbulent correction factor
 φ : Equivalence ratio
 ν : Mole fraction
 ξ : Heat formation

Subscripts

b, u : Burned/unburned gas state
 v : Vented gas state
 o : Standard gas state
 f : Flame state

1. Introduction

Explosions of reactive gases have been investigated for more than a century. These have continuously received considerable attention in connection with the safety aspects. The main attention of safety-related efforts is to prevent the occurrence of accidents. Despite all efforts aimed

* Corresponding Author,

E-mail : kim@kookmin.ac.kr

TEL : +82-2-910-4830; FAX : +82-2-910-4839

School of Mechanical and Automotive Engineering, Kookmin University, 861-1, Chongnung-dong, Songbuk-gu, Seoul 136-702, Korea. (Manuscript Received October 6, 2003; Revised January 2, 2004)

at reducing the probability of the occurrence of explosions, such severe accidents have occurred occasionally. Therefore, it is very important to take suitable methods to reduce these undesirable consequences.

Recent explosion protection methods can be classified into two types; Techniques which come into effect after a deflagration begins are deflagration venting, explosion suppression, isolation and deflagration pressure containment, while other techniques which remove the conditions for a deflagration to start are combustible material concentration control and spark detection/removal (Chatrathi, 1992). For the confined spaces, explosion venting may be efficient in limiting the consequences of an explosion. The ability to predict overpressure arising from explosions is the main key in producing risk assessments and designing explosion relieves.

The simplest technical solution to the problem of protecting systems from the effects of an explosion is the installation of an appropriately sized emergency vent. Various rules and guidelines for designing a safe venting area have been proposed, mainly based on some semiempirical description of the deflagration process (Canu et al., 1990). Most studies explored mathematical solutions of both closed and vented deflagrations, and compared these with experimental data. The basic principle is to model each of the phenomena using simple quantitative theories whenever it is possible; only when this is not possible, suitable relationship containing adjustable parameters should be introduced (Canu et al., 1990 & 1991; Chippett, 1984; Fairweather and Vasey, 1982; Epstein, et al., 1986). In particular, Bradley and Mitcheson (1978a, 1978b) reviewed a great deal of the experimental and analytical work in this area, and established venting guidelines. Numerous analytical, semiempirical, and experimental values for overpressure are compared to their recommended guidelines. In the broad range of vessel sizes ($0.001 \sim 200\text{m}^3$), combustible gases, equivalence ratios, and vessel geometries such as spheres with length to diameter ratios (L/D) of 1, cubes and cylinders with ($L/D > 1$), several analyses have produced over-

pressure that exceed the Bradley-Mitcheson guidelines.

Since hydrodynamic instabilities (Seo, 2003) can arise, leading to the formation of a cellular flame front at some critical expansion ratio (Yun, et al., 2002), the flame is distorted from the spherical shape based on constant flame propagation. Turbulence induced by such process has been recognized as a significant factor but has not been quantified. Therefore, much attention has been paid to the importance.

This study attempts to correlate available experimental data on the venting of gaseous explosions in spherical and cylindrical vessels in terms of the simple theoretical model for the flame propagation in vessel. Theoretical models based on normal one-dimensional undisturbed flame propagation adopted a single value of the turbulence correction factor, so as not to underestimate the violence of the explosion due to the effects of flame acceleration inside the enclosure. Instead of using elaborate numerical models, one can model vented deflagration using the above flame acceleration parameters.

2. Deflagrations in Vessels

A deflagration may be considered as an expansion wave where pressure and density drop and gas velocity increases across the wave. Therefore, the deflagration speed is relative to the moving unburned mixture in front of the flame and cannot be uniquely determined by the given initial conditions. An overall pressure rise of 6 to 10 times to the initial pressure will occur due to the slow burn of most hydrocarbon-air mixtures in an enclosure.

When a combustible gas mixture is ignited, the hot burned gases expand and the pressure rises across the flame front within the whole confined area in the case of a confined explosion. But this expansion will also form a gas flow which may fold the flame, produce turbulence, and initiate combustion instabilities. There are major dynamic effects that can complicate the vessel explosion process. All these contribute to a flame acceleration, and to an increase in the energy-

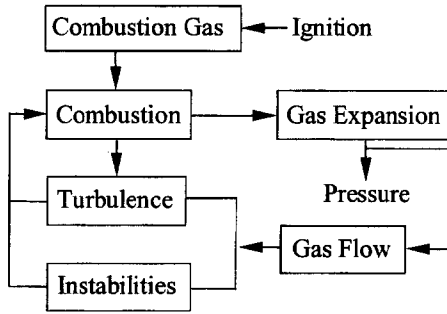


Fig. 1 Flame acceleration as a positive gas dynamic by combustion.

release rate and the pressure.

The combustion can form a gas flow, which acts as a feedback loop on the combustion itself, as sketched in Fig. 1. This coupling mechanism between flame acceleration and gas dynamics is the main problem in gas explosions. The feedback loop shown in Fig. 1 will apply to both the confined and unconfined explosions. The strength of this feedback loop can be such that the flame acceleration will run to the extremes due to turbulence.

3. Model Description

The model is designed under given initial and boundary conditions. Initial conditions refer to the reactant concentrations and their thermodynamic states, possibly their spatial variation inside the vessel, and the characteristics of the ignition source. The boundary conditions include the geometrical details of the vessel such as shape, size, and geometry of the vent openings. The theory of explosion in closed and vented vessels is based on highly idealized model.

A rigid adiabatic vessel of one-dimensional geometry filled with a homogeneous combustible mixture is assumed. The approach to the calculation of the pressure-time history inside these vessels is based on the following set of simplifying assumptions :

1. The flame front speed is sufficiently rapid to cause the thickness of the reaction zone to be small compared with the dimensions of the burned

gas zone. Accordingly, the flame front is treated as a mathematical discontinuity.

2. The gas mixture is initially uniform in composition and is ignited at a central or end point, and the initial mixture composition is stoichiometric.

3. It is assumed that a constant factor, ϕ , which multiplies the laminar burning velocity S_u adequately expresses the effects of increased burning rate due to the flame instabilities.

4. In cylindrical vessels the flame is a spherical segment in shape but in spherical vessel it is a completely spherical shape.

5. When venting occurs the only unburned gases are vented.

6. The burned and unburned gases are expanded or compressed isentropically and instantaneous venting rates are well described by steady-state and isentropic choked flow.

The models of these cases for central and end ignition in closed and vented cylindrical vessels are shown in Fig. 2. The point of origin of the sphere is the ignition location. In the model it is necessary to calculate the flame area and the volume of burnt gas, at each time-step in the numerical solution in order to determine the rate of production of mass of burnt gas.

By simple geometrical calculations, from Fig. 3, the area of the spherical flame segment is expressed by the following equations

$$A_f = 2\pi R d \quad s \geq R \text{ for sphere} \quad (1)$$

$$A_f = 2\pi R (R - \sqrt{R^2 - s^2}) \quad s \leq R \quad (2)$$

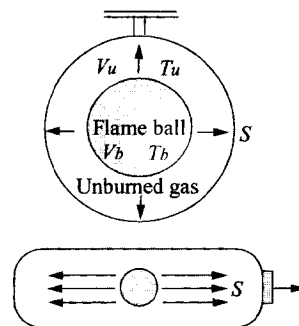


Fig. 2 Illustration of the one-dimensional vessel model. Spherical and cylindrical vessel (with a central ignition source and a vent area).

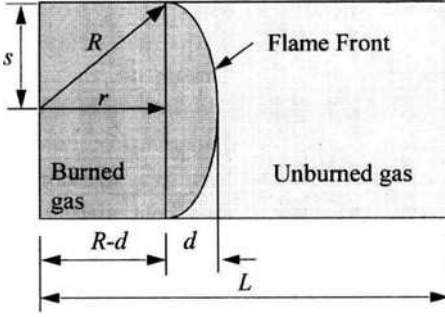


Fig. 3 Geometrical illustration of flame surface for end ignition.

For ignition at a flat end, the term, $\sqrt{R^2-s^2}$, becomes zero. In this limit Eq. (2) reveals that $A_f = 2\pi s^2$. And the volume occupied by the burnt gas can be expressed

$$V_b = 1.5\pi s^2(R - \sqrt{R^2 - s^2}) + \pi s^2(R^2 - s^2) \quad s \leq R \quad (3)$$

In the case of middle ignition, two flame fronts are assumed to proceed in the opposite directions along the axis of the vessel towards the ends of the vessels. The surface area of each flame and volume are double that of ignition at a flat end. The case of a long cylindrical vessel, $\sqrt{R^2 - s^2} \rightarrow \infty$, can be treated by converting the square root term into a series expansion and retaining the first two terms. Thus it yields

$$A_f = 2\pi(\gamma^2 + s^2 - \gamma\sqrt{\gamma^2 + s^2}) \sim 2\pi(\gamma^2 + s^2 - \gamma^2 - 0.5s^2 - \dots) = \pi s^2 \quad (4)$$

The mass conservation equation is:

$$m_0 = m_u + m_b + m_v = \text{const} \quad (5)$$

When this equation is rearranged and differentiated with respect to time, the following mass derivatives are obtained:

$$\frac{dm_u}{dt} = -\frac{dm_b}{dt} - \frac{dm_v}{dt} \quad (6)$$

The constant overall volume is

$$V_0 = V_u + V_b \quad (7)$$

The equation of state for ideal gas behavior applies to both burned and unburned gases, and at any instant the volume of burned gas is given by:

$$V_b = \frac{1}{p} \int_0^{m_b} R_b T_b dm_b \quad (8)$$

The average temperatures in the burned and unburned zones for an adiabatic system are not constant. Also, the temperature of unburned gas increased by compression is in the range of values for a propagating explosion. In accordance with adiabatic pressure changes, the relations between temperature and pressure are:

$$T_u = T_0 \left(\frac{p}{p_0} \right)^{(\lambda_u - 1)/\lambda_u} \quad (9)$$

$$T_b = T_f \left(\frac{p}{p_0} \right)^{(\lambda_b - 1)/\lambda_b} \quad (10)$$

where λ_u and λ_b are the ratios of specific heats at constant pressure. The volume for the unburned and burned gas varies with temperature and pressure for each gas mixture. Equations can be developed using separate values of λ_u and λ_b for simplicity. The approximate mean values of λ_u and λ_b are order of 1.36 to 1.38 and 1.15 to 1.18, respectively, for hydrocarbon-air mixtures. The adiabatic flame temperature T_f used in the first stage of Eq. (10) can be obtained by letting $\Delta H = 0$ in the following equation:

$$\sum_{i=1}^N \nu_i'' \Delta \xi_{f,M_i}^0 - \sum_{i=1}^N \nu_i' \Delta \xi_{f,M_i}^0 - \sum_{i=1}^N \nu_i' (\xi_{Tf} - \xi_{T_0}) + \sum_{i=1}^N \nu_i'' (\xi_{Tf} - \xi_{T_0}) = \Delta H \quad (11)$$

where $\Delta \xi_f^0$ is the standard heat of formation of a substance and $\xi_{Tf} - \xi_{T_0}$ is enthalpy difference. For most stoichiometric fuel-air mixtures, it is in the range of 2000K ~ 2500K.

The expression for the burning velocity S_u is obtained from the equation of mass conservation for the unburned gas. It follows from the definition of laminar burning velocity that

$$S_u = (A_f \rho_u)^{-1} \frac{dm_u}{dt} \quad \text{for laminar conditions.} \quad (12)$$

So, the mass balance of unburned gas is

$$\frac{d\rho_u V_u}{dt} = -A_f \rho_u S_u \phi = -A_f \rho_u S_t \quad (13)$$

where S_t is turbulent burning velocity. By definition, $\phi = S_t/S_u$ depends on the initial turbulence, flame wrinkling, and cell formation due to hydrodynamic instabilities, as shown by Chippett (1984). It is assumed that S_u is a constant valued over the entire cross section of the tube. The most

Table 1 Values used in Eq. (14) for fuel-air stoichiometric mixture.

| Fuel | S_{u0} (m/s) | α | β |
|--------------------------------|----------------|----------|---------|
| CH ₄ | 0.33 | 2.00 | -0.35 |
| C ₃ H ₈ | 0.34 | 2.18 | -0.16 |
| C ₅ H ₁₂ | 0.50 | 1.60 | -0.25 |

widely used expression is a simple power law (Canu et al., 1990 & 1991; Chippett, 1984):

$$S_t = \phi S_u = S_{u0} \left(\frac{T_u}{T_0} \right)^\alpha \left(\frac{p}{p_0} \right)^\beta \phi \quad (14)$$

where T_0 and p_0 are the reference temperature and pressure and S_{u0} is fundamental burning velocity, measured at T_0 and p_0 , and α and β are empirical parameters. Values of S_{u0} , α and β are summarized in Table 1 and ϕ is a turbulent factor to account for any initial stirring or movement of the gas mixture. For quiescent mixtures ϕ is 1.0.

The mass rate of discharge from the confining volume to the surrounding atmosphere via the vent is given by the standard orifice equations.

$$\frac{dm_v}{dt} = \rho_v A_v S_v \quad (15)$$

Two expressions at exit are possible, depending on whether the discharge velocity is subsonic or sonic. If the pressure ratio p/p_0 is less than the critical pressure ratio, $0.5(\lambda+1)^{\frac{\lambda}{\lambda-1}}$, venting is subsonic and discharge velocity becomes

$$S_v = C_d \sqrt{\frac{\lambda p}{\rho_u} \left(\frac{\lambda+1}{2} \right)^{\frac{1+\lambda}{1-\lambda}}} \quad (16)$$

If p/p_0 is greater than the critical pressure ratio, venting is sonic and it becomes

$$S_v = C_d \sqrt{\frac{2\lambda p \rho_u}{\lambda-1} \left(\frac{p_0}{\rho_u} \right)^{\frac{2}{\lambda}} \left(1 - \frac{p_0}{p} \right)^{\frac{\lambda-1}{\lambda}}} \quad (17)$$

in which C_d is the discharge coefficient.

4. Computational Procedure

The algorithm for this model was constructed as the set of equations to solve for the pressure development (deflagration explosions) of the hydrocarbon thermodynamic properties of the combustion system. The analysis for this model

requires a selection of a number of parameters: defining the nature of the gas mixture, the characteristics of the environment, the geometry of the enclosure, and the controls to be applied to the step size in the numerical solution. The program starts the calculations with the required thermodynamic properties of gas mixture. A step by step method of calculation is used to model the combustion process in the system at each increment of flame propagation. The composition is assumed to attain equilibrium instantaneously during expansion at each time step. The unburned and burned volume will be calculated in accordance with the flame propagation and burning velocity. The modes of the ignition source are considered in the program. Mixture compositions and flame-temperatures were calculated for adiabatic constant volume combustion. The heat of combustion is derived from the enthalpy of formation of the species and allows the reaction to reach the equilibrium compositions. From the results of the calculated pressure and temperature, unburned and burned gas mass and density are calculated. These calculated values of physical properties at each step are compared with the total mass to determine their accuracy. If there is no significant numerical difference in the mass conservation the values are adopted for that particular time step. The calculations do not stop until the flame position has been reached at the end point vessel limits. The total combustion time can be obtained by adding the time for each burned mass step.

The instantaneous flame properties-adiabatic flame temperature, species concentration, ratio of specific heats, sonic velocity, gas constant on a mass basis, and density-are calculated in the usual way at each increment in flame distance from ignition source. This is simply achieved by equating initial and final enthalpies of reactants and products using JANAF thermodynamic data (Gardiner Jr., 1984).

5. Computational Results

In order to estimate reasonable pressure values during an explosion, several sets of experimental

data have been examined with different turbulent factors, ϕ . Based on such data, the model reliability is established over a range of conditions, and the values of its adjustable parameters are obtained, through the below procedure, for closed and vented vessels.

5.1 Closed vessel explosion

The numerical calculation was first performed to simulate the experimental conditions examined by Garforth and Rallis (1976, 1978), in which a small-sized spherical vessel is used. A stoichiometric methane-air mixture was ignited in a spherical vessel of 0.1602m at the initial conditions $p_0=1$ atm, and $T_0=292.1$ K. To compare the present analysis with the experimental data (Garforth, 1976; Garforth and Rallis, 1978) and calculated data (Bradley and Mitcheson, 1976; Takeno and Iijima, 1979), the pressure-time relations in Fig. 4 were solved with the empirical burning velocities of the stoichiometric methane-air mixture, as a function of pressure and the unburned gas temperature. The comparison with the experimental and other calculated data in Fig. 4 shows that no non-unity turbulence factor is needed in small vessels. The model prediction with $\phi=1.0$ is in reasonable agreement with the experimental data. In this case the flame front does not become distorted; there are no factors that make the flame accelerate. The time indicated by the four vertical lines intersecting the horizontal axis of Fig. 4 is the time needed to arrive at

the final pressure, 9.001 atm with respect to Garforth and Rallis' data. The unburned gas is considered isotropic, but the isentropic changes of each burned gas element are evaluated individually. Thus, the burned gas is anisotropic. Anisotropy of the burned gas increases the final pressure value in closed deflagrations.

Figure 5 shows burning velocities as a function of the pressure in which the effect of the unburned gas temperature is increased. It seems that the discrepancy in the burning velocity affects significantly the calculated pressure history. Calculated solutions in closed vessels show that they are very sensitive to the numerical value of burning velocity.

A comparison of flame position between the experimental and calculated results of the present

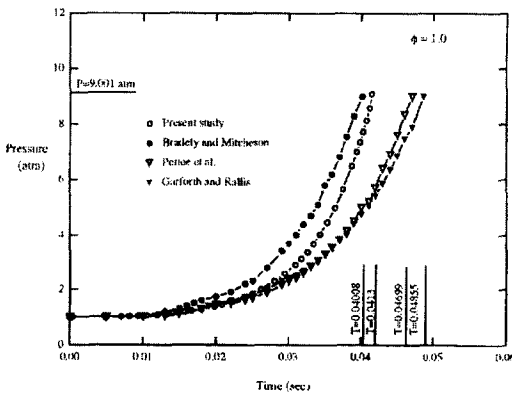


Fig. 4 Predicted pressure-time curves for empirical burning velocities.

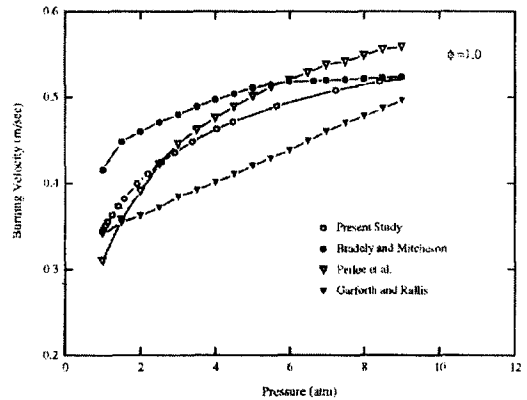


Fig. 5 Variation with the pressure of burning velocities for stoichiometric methane-air mixture.

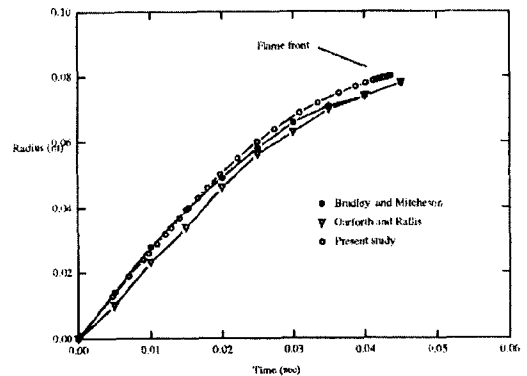


Fig. 6 Predicted flame radius with the same conditions as shown in Fig. 4.

study is presented in Fig. 6. The general prediction of flame positions is in fair agreement with experimental data (Garforth and Rallis, 1978), but the discrepancy with other calculated data (Bradley and Mitchenson, 1976) increases slightly with increasing flame radius.

In spherical closed vessels, the comparison with experimental data shows that the turbulence correction factor is $\phi \approx 1.0$ in small size vessels. In medium and large size vessels, a non-unity turbulence correction factor is needed due to flame instability. As the size of the vessel increases, the turbulence correction factor increases slightly for the large size as shown in Fig. 7 for a vessel of 1.936m diameter at the initial conditions $p_0=3$ atm, $T_0=298$ K, for 10% CH_4 -air mixture. The results of the present calculation with $\phi=1.0$ do not agree with other experimental and calculated data (Canu et al., 1990) as shown in Fig. 7. Through trial and error method, two values are used in this work ($\phi_1=1.0$, $\phi_2=1.6$). By using these two ϕ values at the appropriate time, good agreement with the experimental data (Canu et al., 1990) in Fig. 7 is obtained. The comparison shows that the change of burning velocity due to the onset of instability occurs at 0.78m from the central ignition point (0.32s) obtained by using the experimental information.

Figure 8 shows results for another condition of

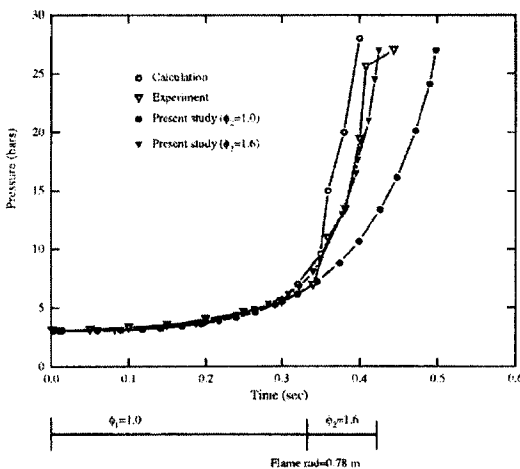


Fig. 7 Pressure-time curves for closed vessel explosion in a medium size vessel ($D=1.936$ m).

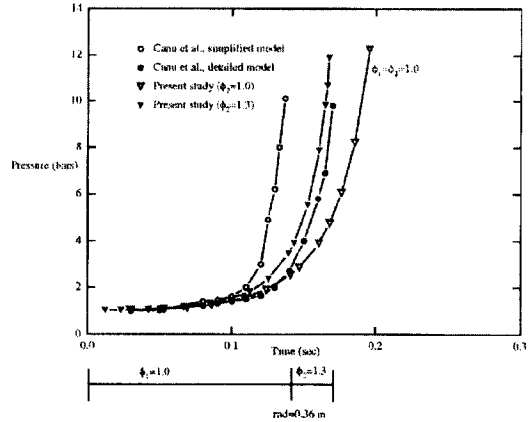


Fig. 8 Calculated pressure-time curves for stoichiometric C_3H_8 -air mixture in closed spherical vessel ($D=0.8$ m).

0.268m^3 initial volume, and 0.8m diameter, where a medium-size spherical vessel contains a stoichiometric propane-air mixture. In this case the corrected turbulence factors, ($\phi_1=1.0$, $\phi_2 \approx 1.3$) are also shown to have good agreement with the experimental data. The comparison shows that a burning velocity after change due to the onset of instability occurs at the 0.36m from central ignition point (0.14s). As shown in the two medium-size vessel studies, the values of ϕ_2 show a range of 1.3 to 1.6 in the case of medium-size or larger closed spherical vessels. As shown in the previous small-sized closed vessel study, $\phi_1=1.0$ is assumed during quiescent condition. However, $\phi_2=1.3$ to 1.6 is assumed to describe flame acceleration effects. That is, the values of ϕ_2 can be determined by the comparison with the experimental data.

5.2 Vented vessel explosion

Explosion venting has been already considered as the best role in safety measures. It has the effect of stopping or at least retarding the pressure increases within vessels. Unfortunately it has an enhancing effect on the rate of flame propagation. The pressure-time curve after vent opening is strongly dependent on the vent area. The effect of flame turbulence also becomes predominant.

The double turbulence correction factors, (ϕ_1 , ϕ_2), for the present model of hydrocarbon-air

mixture explosion and venting phenomena in spherical vessels, have been adjusted against the experimental results dealing with spherical cases. The calculated pressure-time curves for vented explosions were obtained for 9.5% methane-air in spherical vessels (1.9m^3) with initial conditions, $p_0=3.103$ bars, $T_0=298\text{K}$ and central ignition. The experimental data (Bradley and Mitchenson, 1978b) in Figs 9 and 10 are selected to compare the calculated values. Two calculations, Chippett's and Canus (1984, 1990 and 1991) works are shown for each experiment, along with the results of this research. For vent opening pressures with $p_v=4$ bars and 6.205 bars respectively, they show that peak pressure

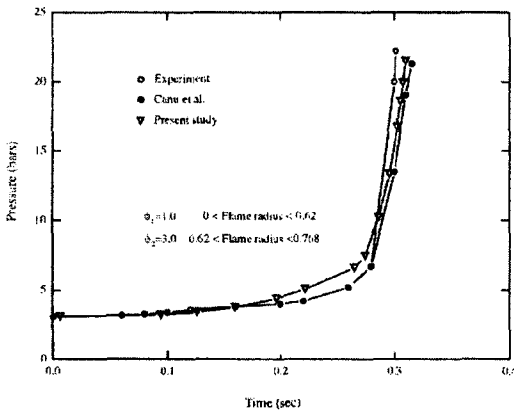


Fig. 9 Comparison of calculated and measured pressure-time curves for vented deflagration when $p_v=6.205$ bars.

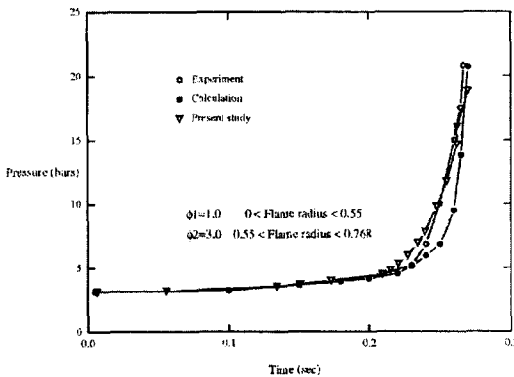


Fig. 10 Comparison of calculated and measured pressure-time curves for vented deflagration when $p_v=4$ bars.

increases slightly, and the time to reach peak pressure increases as vent opening pressure increases. The comparison shows that a burning velocity changes due to the strong turbulence occurring while a vent cover bursts at 0.62m and 0.55m from the central ignition point respectively.

Turbulence correction factors of $\phi_2=2.4$ to $\phi_2=3.0$ were found to yield the best correlation to the peak pressure data. Figure 11 shows the predicted peak pressure together with the pressure predicted by others for stoichiometric C_3H_8 -air mixture, initial atmospheric pressure, and spherical vessel (0.268m^3). These peak pressures require a much low value of $\phi_2=2.4$ to give the best agreement with the other calculated data. The value for ϕ_1 of 1.0 has been used prior to the onset of instability in Fig. 11. The instant at which the instabilities occurred in the experiments is not known. It is assumed that instability has set in whenever a sudden and large change in the value ϕ was required to match the calculated and experimental pressure transients. A sudden change in the flame speed is indicated at 0.29m for the vent opening pressure of 1.5bars.

The change in the flame speed depends on a strong turbulence generation when the vent area opens. It only depends on combustion instability and turbulence near the end wall in a closed system. Although all the details of the pressure transients before and after the vent has opened are

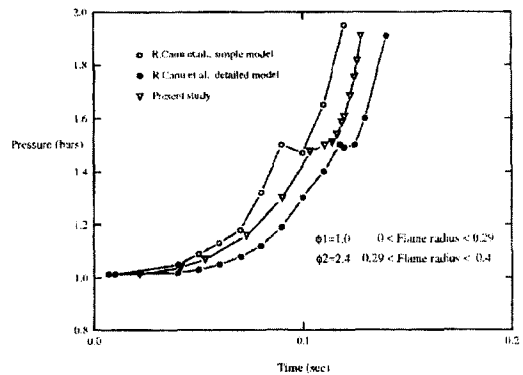


Fig. 11 Calculated pressure-time curves for stoichiometric C_3H_8 -air mixture in vented spherical vessel ($D=0.8\text{m}$), $A_v=5.391 \times 10^{-2}\text{m}^2$, $p_v=1.5$ bars.

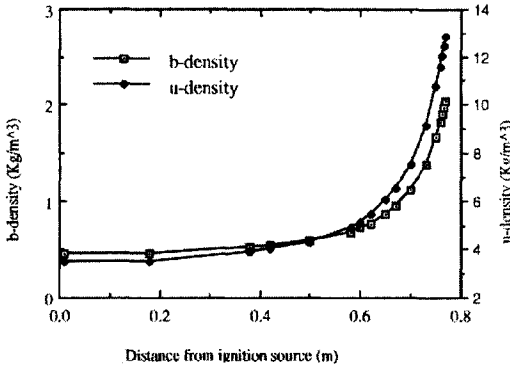


Fig. 12 Calculated density of unburned and burned gases with regard to the distance of flame front from ignition source.

not predicted, the agreement between the calculated and measured transients is very good. The value of $\phi=1.0$ is required to match the initial part of the curves. In the results, a turbulence correction factor of $\phi_2 \sim 3.0$ can be expected to yield reasonable correlations of peak pressure during hydrocarbon-air explosions in sonic vented, and nearly spherical vessels.

Figure 12 presents the density distribution at several locations during flame propagation, for the same conditions as in Fig. 10. The deflagration flame separates two gases of markedly different density with $\rho_u \sim 7\rho_b$. Figure 13 shows the effect on the peak pressure as the discharge coefficient varies from 0.6 to 1.0 for deflagrations

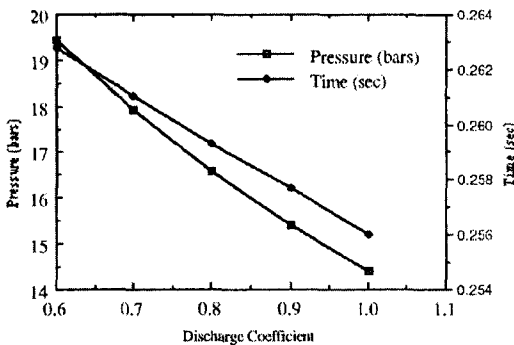


Fig. 13 Effect of discharge coefficient on the maximum deflagration pressure, and time to reach the maximum deflagration pressure in vented spherical vessel ($D=0.8\text{m}$), $A_v=5.391 \times 10^{-2}\text{m}^2$, $p_v=1.5\text{bars}$.

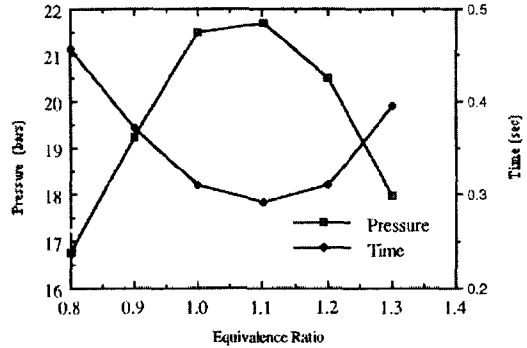


Fig. 14 Effect of equivalence ratio on the maximum deflagration pressure and time to reach the maximum deflagration pressure in vented spherical vessel ($D=1.536\text{m}$), $A_v=0.0324\text{m}^2$, $p_v=4\text{bars}$.

in spherical vessel with the same initial conditions used in Fig. 11, along with the same vent opening pressure. The peak pressure decreases greatly, and time to reach the peak pressure also decreases as discharge coefficient increases. A choice of discharge coefficient is clearly important in matching calculated results with experimental data (Chippett, 1984).

The methane concentration has a strong influence on the peak pressure, as shown in Fig. 14. This applies to the peak pressure for which the maximum occurs at the equivalence ratio, 1.1, but the time to reach peak pressure is the lowest at the same condition. This means the maximum pressure should be obtained at 1.1 because the maximum value of burning velocity, S_u , is obtained at an equivalence ratio of around 1.1. This suggests a preventive technique to reduce peak pressure through combustible material concentration control.

Calculated pressure-time curves for vented explosions were obtained for 5% C_3H_8 -air in cylindrical vessels ($3.2 \times 10^{-2}\text{m}^3$) with $L=0.439\text{m}$, $D=0.3048\text{m}$, $T_0=298\text{K}$, end ignition, $p_0=2.03, 4.05\text{bars}$, vent opening pressures and p_v in the range of 2.46 to 25.83bars. Venting area, A_v is varied in the range of 9.91 to 25.33(m^2)/100(m^3) x cylindrical vessel volume (m^3). The experimental data of Cousins and Cotton (1951) were used to be compared with the present results.

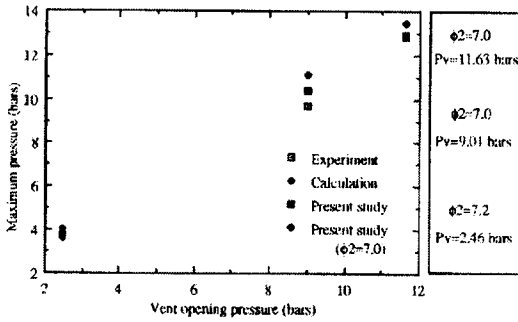


Fig. 15 Effect of vent opening pressures on explosion pressure for 5% Propane-air mixture ($3.2 \times 10^{-2} \text{m}^3$) when $p_0 = 2.03 \text{bars}$ and vent ratio $= 25.33 \text{m}^2/100 \text{m}^3$.

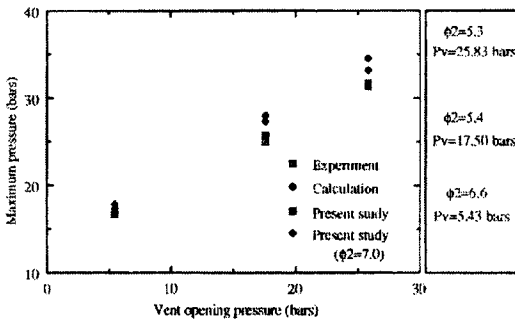


Fig. 16 Effect of vent opening pressures on explosion pressure for 5% Propane-air mixture ($3.2 \times 10^{-2} \text{m}^3$) when $p_0 = 4.05 \text{bars}$ and vent ratio $= 9.91 \text{m}^2/100 \text{m}^3$.

Increasing the vent opening pressure from 2.46 to 25.83 bars has a significant influence on the peak pressure as shown in Figs. 15 and 16. Although Figs. 15 and 16 do not have results showing some information between the peak pressure and the vent ratio at the same vent opening pressure, increasing the vent ratio has some influences in spherical cases as shown in Chippett's results (1984). The best estimated value $\phi_2 \approx 7.0$ is obtained by being compared with experimental data for small L/D cylindrical vessel, which makes the peak pressure results within 20% of the experimental data as well as other calculated data (Cousins and Cotton, 1951).

6. Conclusion

The mathematical model, which accounts for

each of the main physical-chemical phenomena occurring in a closed or a vented deflagration, has been simplified through suitable assumptions for easy application. The model incorporates turbulence by simply multiplying the laminar burning velocity by one or two different turbulence factors ϕ_1 . The value of ϕ is determined by the experimental data of other researchers.

As the size of the vessel increases a non-unity turbulence correction factor is needed due to flame instabilities. For spherical vessels, the extra turbulence produced by venting requires the larger value of ϕ_2 than unvented vessel. As the L/D ratio increases, the value of ϕ_2 increases proportionately over the value needed for a spherical vessel at the same initial conditions. The present turbulence parameter results provide a convenience tool with which the magnitude of the deviation of actual behavior from idealized laminar combustion venting in deflagration explosion can be readily determined.

References

- Bradley, D. and Mitchenson A., 1976, "Mathematical Solutions for Explosions in Spherical Vesels," *Combustion and Flame*, Vol. 26, p. 210.
- Bradley, D. and Mitchenson A., 1978a, "The Venting of Gaseous Explosions in Spherical Vessels I," *Combustion and Flame*, Vol. 32, p. 221.
- Bradley, D. and Mitchenson A., 1978b, "The Venting of Gaseous Explosions in Spherical Vessels II," *Combustion and Flame*, Vol. 32, p. 237.
- Canu, P., Rota, R. Carra, S., and Morbidelli, M., 1990, "Vented Gas Deflagrations ; A Detailed Mathematical Model Tuned on a Large Set of Experimental Data," *Combustion and Flame*, Vol. 80, p. 49.
- Canu, P., Rota, R., Carra, S. and Morbidelli, M., 1991, "Vented Gas Deflagration Modeling : A Simplified Approach," *Combustion and Flame*, Vol. 85, p. 319.
- Chatrathi, K., 1992, "Deflagration Protection of Pipes," *Plant/operation Progress*, Vol. 11-2, p. 116.

- Chippett, S., 1984, "Modeling of Vented Deflagrations," *Combustion and Flame*, Vol. 55, p. 127.
- Cousins, E. W. and Cotton, P. E., 1951, "Design Closed Vessels to Withstand Internal Explosions," *Chemical Engineering*, Aug., p. 133
- Epstein, M., Swift, I. and Fauske, H. K., 1986, "Estimation of Peak Pressure for Sonic-Vented Hydrocarbon Explosions in Spherical Vessels," *Combustion and Flame*, Vol. 66, p. 1.
- Fairwather, M. and Vasey, M. W., 1982, "A Mathematical Model for the Prediction of Overpressures Generated in Totally Confined and Vented Explosions," *19th Symposium International on Combustion, The Combustion Institute*, p. 645.
- Gardiner Jr., W. C., 1984, *Combustion Chemistry*, Springer-Verlag, New York.
- Garforth, A. M., 1976, "Unburnt Gas Density Measurement in a Spherical Combustion Bomb by Infinite-Fringe Laser Interferometry," *Combustion and Flame*, Vol. 26, p. 343.
- Garforth, A. M., and Rallis, C. J., 1978, "Laminar Burning Velocity of Stoichiometric Methane-Air : Pressure and Temperature Dependence," *Combustion and Flame*, Vol. 31, p. 53.
- Seo, S., 2003, "Combustion Instability Mechanism of a Lean Premixed Gas Turbine Combustor," *KSME International Journal*, Vol. 17, p. 906
- Takeno, T. and Iijima, T., 1979, "Theoretical Study of Nonsteady Flame Propagation in Closed Vessels," *AIAA, Aug.*, Vol. 119, p. 578.
- Yun, K., Lee, S. and Sung, N., 2002, "A Study of the Propagation of Turbulent Premixed Flame Using the Flame Surface Density Model in a Constant Volume Combustion Chamber," *KSME International Journal*, Vol. 16, p. 564